JOURNAL OF MATERIALS SCIENCE **40** (2005) 3897 – 3903

Pitch-matrix composites for electrical, electromagnetic and strain-sensing applications

S. WEN, D. D. L. CHUNG
Composite Materials Research Laboratory, University at Buffalo, Buffalo, NY 14260-4400, USA

Pitch-matrix composites for deicing, electromagnetic shielding and strain sensing have been developed by using carbon fiber (discontinuous) and carbon black as electrically conductive fillers. A composite with carbon fiber (5 vol%) as the sole filler is effective for strain sensing, which functions by the electrical resistivity increasing reversibly with tensile strain. A composite with carbon fiber (3.4 vol%) and carbon black (1.5 vol%) is less effective for strain sensing and is lower in tensile strength, modulus and ductility, but it is lower in the electrical resistivity. A composite with carbon black (7 vol%) as the sole filler is very high in resistivity, but exhibits high storage modulus. Either carbon fiber or carbon black as filler increases the storage modulus, decreases the resistivity, renders the ability to provide EMI shielding and increases the softening temperature.

1. Introduction

Pitch-matrix composites (e.g., asphalt) are widely used for pavements, roofing, sealing and related structural applications. However, the simultaneous use of these materials for structural and non-structural functions is desired for the purpose of providing smart structures and alleviating the high cost, low durability and design complexity associated with using separate structural and non-structural components in the same structure. This paper addresses pitch-matrix composites for electrical and self-sensing applications.

An electrical application pertains to resistance heating, which is relevant to pavement deicing, particularly the deicing of airport runways, bridges and highways. Resistance heating means Joule heating, i.e., heating due to the passing of a current through a resistor. The resistor obviously must be electrically conductive. A resistor with a high resistance allows only a small current to go through, unless the voltage is undesirably high. A small current results in little heating. Therefore, the resistivity of the material of the heating element should be sufficiently low. As pitch itself is not conductive, pitch-matrix composites that are rendered conductive by the use of conductive fillers are needed for resistance heating.

Another electrical application pertains to electromagnetic interference (EMI) shielding, which refers to the blocking of electromagnetic radiation, such as radio frequency waves from cellular phones. The radiation can interfere the function of computers, pacemakers, transformers and other electronic devices. Asphalt that is capable of shielding is particularly valuable for the protection of transformers and other electronics that are housed in concrete vaults underground. It is also valuable for use as a coating on concrete for providing shielded structures. In spite of these applications, the shielding effectiveness of pitch-matrix composites have not been investigated previously. Electrically conductive materials are usually effective for shielding, due to their ability to reflect the radiation. Thus, conductive pitch-based materials are evaluated in this work for shielding.

Although electrostatic discharge protection (anti-static) is not explicitly addressed in this paper, it is expected that pitch-matrix composites of high conductivity will be attractive for anti-static floors and pavements.

Self-sensing refers to the ability of a structural material to sense its own attributes, such as strain and damage. Self-sensing is in contrast to the use of embedded or attached sensors, which suffer from high cost, low durability, limited sensing volume and, in the case of embedded sensors, loss of mechanical properties. The self-sensing of strain is valuable for weighing (as strain relates to stress, which in turn relates to the force), traffic monitoring, border monitoring, and structural vibration control (as strain relates to vibration). The self-sensing of compressive stress has been reported in a pitch-matrix composite containing graphite particles; the resistance increased with increasing compressive stress in a partly reversible fashion, though the repeatability of this piezoresistive effect (effect in which the electrical resistivity changes with stress or strain) was poor [1]. The self-sensing of compressive stress has also been reported in a composite with a polyethylene matrix and containing carbon black; the resistance decreased with increasing compressive stress [2]. By using carbon fiber instead of graphite particles, this paper provides an improved pitch-matrix composite for the self-sensing of strain and damage.

Since pitch itself is a polymer which is not conductive and sand, in the case of asphalt, is also not conductive, fillers that are conductive are used to provide low resistivity to pitch-matrix composites. Fillers that have been used in prior work for this purpose include graphite particles [1, 3, 4], carbon fiber [4–6], steel fiber [4] and carbon black [7].

In general, fibers are more attractive than particles as electrically conductive fillers. This is due to the large aspect ratio and the consequent increased chance of forming a continuous conduction path—a situation known as percolation. The percolation threshold is the conductive filler volume fraction above which a continuous conductive path exists. At a given filler volume fraction, the percolation threshold tends to decrease with increasing aspect ratio of the filler.

The combined use of fibers and particles as conductive fillers can be attractive, since particles tend to be less expensive than fibers and fibers tend to promote percolation. In case of particle agglomerates that are highly compressible, as in the case of carbon black, the particle agglomerates can, upon compression, become filamentous and touch one another, thereby promoting percolation. Therefore, this work included investigation of the combined use of carbon fiber and carbon black for attaining pitch-matrix composites of low resistivity. For the sake of comparison, this work includes investigation of the use of carbon fiber as the sole filler and of carbon black as the sole filler.

2. Experimental methods

2.1. Materials

The pitch used was 170 Petroleum Pitch from Crowley Tar Products Company, Inc. (New York, NY). Its density was 1.21 g/cm^3. The aggregate used was natural sand of density 2.88 g/cm^3 (as measured by using the Archimedes' Principle). The particle size analysis of the sand (all passing #25 U.S. sieve, 0.710 mm aperature 99.9% SiO_2) is shown in Fig. 1 of Ref. 7. The sand/pitch ratio was 1.0.

The carbon black was Vulcan XC72R GP-3820 from Cabot Corp., Billerica, MA. This carbon black was chosen due to its electrical conductivity and easy dispersion. It was in the form of porous agglomerates of carbon particles of average size 30 nm, a nitrogen specific surface area of 254 m^2/g, a volatile content of 1.07%, a maximum ash content of 0.2% and a density of 1.7–1.9 g/cm^3.

The carbon fiber was based on isotropic pitch, with a diameter of 15 μm, a nominal length of 5 mm and a density of 1.6 g/cm^3, as provided by Ashland Petroleum Co., Ashland, KY.

Pitch was first melted in a steel container by using a hot plate at 120°C and mixed in the molten state by hand for 10 min with a chosen amount of filler (i.e., carbon black and carbon fiber, at ratios and total filler volume fractions shown in Table I). Sand, if applicable, was added to the mix. The mixture was allowed to cool to room temperature. After solidification, the pitch-based material was ground by hand into composite particles of size around 0.1–1 mm. These particles were placed in a 160 × 15 mm steel mold cavity and then melted at 120°C for 15 min by using a hot plate. Immediately after melting, a matching steel piston was placed in the mold cavity. The pressure, as provided by a combination of piston weight and manual force, ranged from 0.09 to 0.36 MPa. The higher the filler content, the greater was the pressure used. Subsequent cooling, demolding and then cutting resulted in specimens of size 60 × 10 × 2 mm. In the case of pitch without filler, the procedure was the same except that the pitch particles placed in the mold were obtained by crushing the solid pitch without prior melting.

2.2. Electrical resistivity measurement

The electrical resistivity was measured by using the four-probe method. The specimens were of size 60 × 10 × 2 mm. The outer two electrical contacts (40 mm apart) were for passing current and the inner two electrical contacts (20 mm apart) were for measuring the voltage. Each of the two pairs of electrical contacts was symmetrically positioned relative to the mid-point of the length of the specimen. Silver paint in conjunction with copper wire was used for the electrical contacts. Each electrical contact was around the entire perimeter of the specimen in a plane perpendicular to the length of the specimen. Six specimens of each type were tested.

2.3. EMI shielding effectiveness measurement

The shielding effectiveness is the attenuation upon transmission. On the other hand, a low attenuation upon reflection corresponds to a high reflectivity. In case that the reflection is the dominant mechanism for shielding, a high attenuation upon transmission correlates with a low attenuation upon reflection.

The attenuations upon reflection and transmission were measured using the coaxial cable method (the transmission line method (Fig. 1)). The set-up consisted of an Elgal (Israel) SET 19A shielding effectiveness tester with its input and output connected to

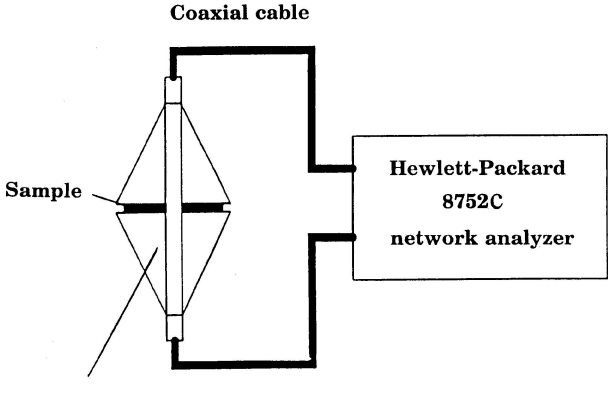

Figure 1 Set-up for measuring the electromagnetic interference shielding effectiveness.

TABLE I Properties of pitch and pitch-matrix composites with various weight ratios of carbon fiber to carbon black

Total filler content		Ratio of carbon fiber to carbon black					
vol%	% by weight of pitch	Weight ratio	Volume ratio	Softening temperature (°C)	Electrical resistivity (Ω·cm)	Storage modulus at 1 Hz (GPa)	Tan δ at 1 Hz
5.03	7.0	1:0	1:0	46.3	363 ± 33	2.01	0.452
4.92	7.0	1:0.25	1:0.22	/	28.6 ± 2.4	/	/
4.85	7.0	1:0.50	1:0.44	43.9	12.1 ± 0.8	2.05	0.349
4.76	7.0	1:1	1:0.89	/	71.3 ± 5.5	/	/
4.67	7.0	1:2	1:1.77	/	447 ± 43	/	/
4.60	7.0	1:4	1:3.55	/	$2{,}450 \pm 290$	/	/
5.40[d]	/	0:1	0:1	44.9	[a]	1.86	0.114
7.00[d]	/	0:1	0:1	55.6	$276{,}000 \pm 38{,}000$	3.04	0.073
0[d]	0	/	/	40.1	[a]	1.33	0.152

[a]Too high to be measured.
[b]Specimen thickness = 4.40 mm.
[c]Specimen thickness = 4.35 mm.
[d]From Ref. 7.

a Hewlett-Packard (HP) 8510A network analyzer. An HP APC-7 calibration kit was used to calibrate the system. The frequency was either 1.0 or 1.5 GHz. The sample placed in the center plane of the tester (with the input and output of the tester on the two sides of the sample) was in the form of an annular ring of outer diameter 97 mm and inner diameter 29 mm. The sample thickness was measured for each specimen. The average thickness was 4.4 mm. Silver paint was applied at both inner and outer edges of each specimen and at the vicinity of the edges in order to make electrical contact with the inner and outer conductors of the tester [9]. Three specimens of each type were tested.

2.4. Self-sensing evaluation and tensile testing

Tensile testing was performed using a Sintech 2/*D* screw-action mechanical testing system under cyclic tensile loading at a stress magnitude of either 1.1 or 2.2 MPa. After cyclic loading at a particular stress amplitude, tensile testing was performed during static loading up to failure. The loading speed was 0.5 mm/min. Three specimens of each composition were tested. During tensile testing, the longitudinal strain was measured by using a strain gage attached to the center of one of the largest sides of the specimen ($150 \times 12 \times 5$ mm). Simultaneously with mechanical testing, the longitudinal DC electrical resistance was measured using the four-probe method. The longitudinal resistance refers to the resistance along the stress axis. The electrical contacts were made by silver paint (in conjunction with copper wire) applied along the whole perimeter in four parallel planes perpendicular to the stress axis. The inner two contacts (50 mm apart) were for voltage measurement, while the outer two contacts (70 mm apart) were for passing a current. The longitudinal strain and resistance were measured simultaneously for each specimen. A Keithley (Keithley Instruments Inc., Cleveland, OH) 2001 multimeter was used. The volume resistivity was calculated from the measured resistance, measured longitudinal strain and calculated transverse strain (Poisson effect). Three specimens of each composition were tested to ascertain reproducibility of the trends reported here.

2.5. Softening temperature measurement

The softening temperature was measured by performing thermal mechanical analysis (TMA) in the penetration mode at a compressive stress of 1415 Pa (as applied through a quartz probe with a flat tip of diameter 3 mm), using a Perkin-Elmer Corp. (Norwalk, CT) Model TMA 7E thermal mechanical analyzer. The heating rate was 2°C/min. The sample size was 8×5 mm in the plane perpendicular to the stress direction and 3 mm in the stress direction, as obtained by cutting the specimens described above. The softening temperature was taken as the intersection of the extrapolation of the baseline with the tangent of the TMA curve (i.e., curve of the fractional change in dimension in the stress direction vs. temperature) in the high temperature regime. For examples of TMA curves, please refer to Fig. 1 of Ref. 7. Three specimens of each type were tested.

2.6. Dynamic mechanical testing

The dynamic mechanical properties under flexure were studied at controlled loading frequencies (1.0 Hz) and room temperature (20°C), using a Perkin-Elmer Corp. (Norwalk, CT) model DMA 7E dynamic mechanical analyzer. Measurements of storage modulus were made at various constant frequencies. The specimens were in the form of beams ($160 \times 5.0 \times 3.5$ mm) under three-point bending, such that the span was 150 mm. The loads used were all large enough so that the amplitude of the specimen deflection was from 6.0 to 9.0 μm (over the minimum value of 5 μm required by the equipment for accurate results). The loads were set so that each different type of specimen was always tested at its appropriate stress level. Six specimens of each type were tested.

TABLE II Electromagnetic behavior of pitch-matrix composites

Ratio by weight of carbon fiber to carbon black	Specimen thickness (mm)	Attenuation upon transmission[a] (dB)		Attenuation upon reflection (dB)	
		1.0 GHz	1.5 GHz	1.0 GHz	1.5 GHz
1:0	4.40 ± 0.53	25.6 ± 2.08	27.4 ± 3.15	1.35 ± 0.16	1.81 ± 0.19
1:0.50	4.35 ± 0.47	23.1 ± 1.86	23.7 ± 2.14	1.40 ± 0.11	1.99 ± 0.16

[a]Same as EMI shielding effectiveness.

3. Results and discussion

3.1. Electrical resistivity

Table I shows the electrical resistivity of various pitch-matrix composites. The resistivity decreased with increasing carbon black proportion, reaching a minimum resistivity of 12 Ω·cm at a weight ratio of 1:0.50 for the ratio of carbon fiber to carbon black. Beyond this proportion of carbon black, the resistivity increased with increasing carbon black proportion. The resistivity for the case of carbon fiber as the sole filler was much lower than that for the case of carbon black as the sole filler. However, combined use of carbon fiber and carbon black in the weight ratio 1:0.25, 1:0.50 or 1:1 resulted in lower resistivity than the value resulted from the use of carbon fiber as the sole filler. The optimum weight ratio was 1:0.50 for attaining the lowest resistivity.

3.2. EMI shielding effectiveness

The electromagnetic behavior of the pitch-matrix composites corresponding to the first and third entries of Table I is shown in Table II. The EMI shielding effectiveness was slightly higher (due to slightly higher reflectivity, as indicated by a lower attenuation upon reflection) for the composite with carbon fiber but without carbon black, than that containing carbon fiber and carbon black in the weight ratio 1:0.50. This is in spite of the higher resistivity of the composite without carbon black. Thus, the combined use of carbon fiber and carbon black is less effective for shielding than the use of carbon fiber alone. This result is consistent with the fact that electrical connectivity is much more important for conduction than for shielding. The greater connectivity imparted by carbon black helped the conductivity but did not help the shielding. Due to the low cost of carbon black compared to carbon fiber, the combined use of carbon fiber and carbon black for shielding remains attractive.

3.3. Self-sensing and tensile behavior

3.3.1. Composite with carbon fiber as the sole filler

The carbon fiber content is 5.03 vol%. The composite is similar to the one in the first entry of Table I. Fig. 2 shows that the longitudinal resistance increased reversibly with increasing tensile strain in every loading cycle at a stress amplitude of 1.1 MPa. The corresponding resistivity variation is shown in Fig. 3. The resistivity also increased reversibly with strain. The fractional change in resistance per unit strain (i.e., the gage factor) is 3.45 ± 0.72, as shown in Table III.

TABLE III Gage factor of pitch-matrix composites at different tensile stress amplitudes

Ratio by weight of carbon fiber to carbon black			
1:0		1:0.50	
1.1 MPa	2.2 MPa	1.1 MPa	2.2 MPa
3.45 ± 0.72	17.3 ± 3.2	0.63 ± 0.08	1.84 ± 0.13

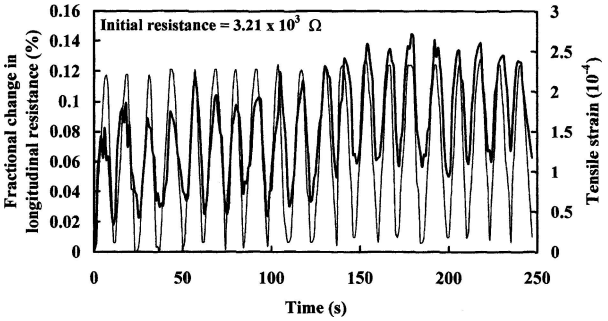

Figure 2 Curves of fractional change in resistance (thick curve) versus time and of tensile strain (thin curve) versus time under cyclic tensile testing at a fixed stress amplitude of 1.1 MPa for the composite with carbon fiber as the sole filler.

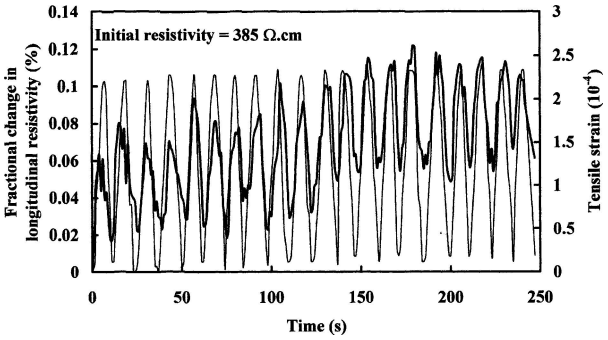

Figure 3 Curves of fractional change in resistivity (thick curve) versus time and of tensile strain (thin curve) versus time under cyclic tensile testing at a fixed stress amplitude of 1.1 MPa for the composite with carbon fiber as the sole filler.

Fig. 4 shows similar behavior at a stress amplitude of 2.2 MPa. Both the resistance and the resistivity (plot not shown) increased reversibly with strain. The gage factor is 17.3 ± 3.2 (Table III). Although the gage factor is much higher at the higher stress amplitude, the signal-to-noise ratio was lower at the higher stress amplitude.

Fig. 5 shows the behavior during static loading up to failure. Fig. 6 shows a magnified view of the portion of Fig. 5 before the abrupt resistance increase, which occurred in Fig. 6 at a strain of 0.06%. The resistivity increased steadily and gradually with increasing strain up to 0.06%, beyond which the resistivity increased abruptly.

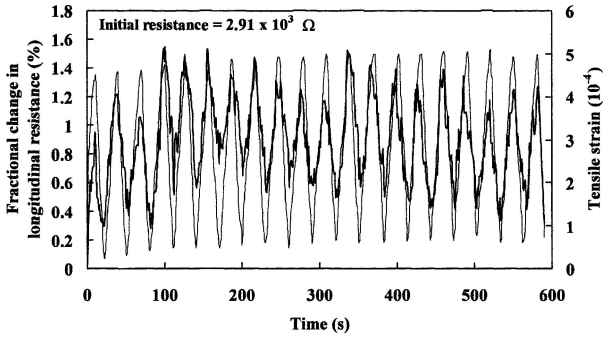

Figure 4 Curves of fractional change in resistivity (thick curve) versus time and of tensile strain (thin curve) versus time under cyclic tensile testing at a fixed stress amplitude of 2.2 MPa for the composite with carbon fiber as the sole filler.

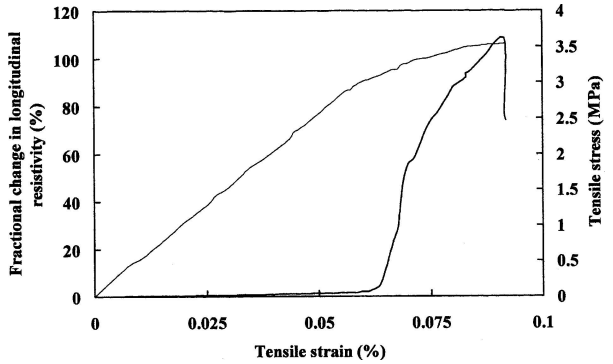

Figure 5 Relationship between stress (thin curve) and strain and that between fractional resistivity change (thick curve) and strain during static tensile testing up to failure for a composite with carbon fiber as the sole filler.

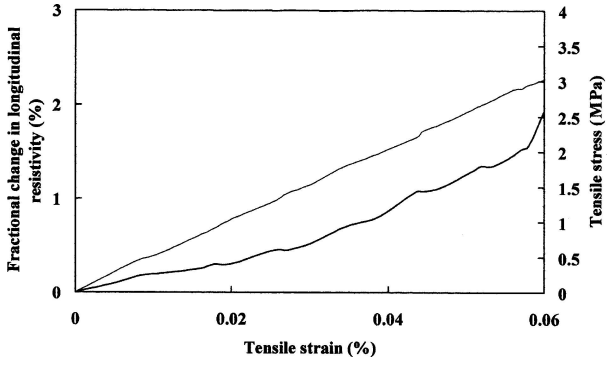

Figure 6 Enlarged view of initial portion of the curve of stress (thin curve) versus strain and that of fractional resistivity change (thick curve) versus strain in Fig. 5.

The tensile properties are shown in Table IV. The stress-strain curve (Fig. 5) was linear up to a strain of 0.06%. It started to deviate from linearity at about the strain (0.06%) corresponding to the start of the abrupt resistivity increase. The deviation from linearity and the abrupt resistivity increase strongly suggest the occurrence of damage.

3.3.2. Composite with carbon fiber and carbon black

The carbon fiber content is 3.36 vol%; the carbon black content is 1.49 vol%. The total filler content is 4.85 vol%. The composite is similar to the one with resistivity 12 Ω·cm in Table I.

TABLE IV Tensile properties of pitch-matrix composites with carbon fiber and/or carbon black

	Ratio by weight of carbon fiber to carbon black	
	1:0	1:0.50
Tensile strength (MPa)	3.55 ± 0.43	3.29 ± 0.30
Tensile modulus (GPa)	4.98 ± 0.54	4.43 ± 0.43
Ductility (10^{-4})	9.20 ± 0.85	8.30 ± 0.77
Stress (MPa)	3.04 ± 0.21	3.10 ± 0.25
Strain (10^{-4}) (at abrupt increase of electrical resistivity)	6.13 ± 0.48	7.21 ± 0.52

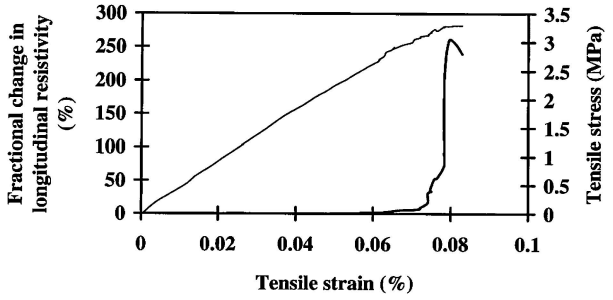

Figure 7 Variation of the fractional change in longitudinal resitivity (thick curve) with tensile strain and of the tensile stress (thin curve) with tensile strain during static loading up to failure for the composite with both carbon fiber and carbon black.

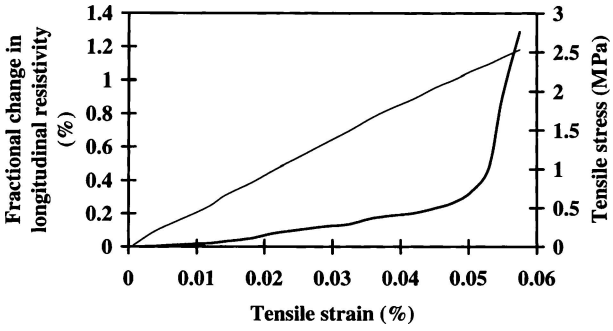

Figure 8 Variation of the fractional change in longitudinal resitivity (thick curve) with tensile strain and of the tensile stress (thin curve) with tensile strain during static loading up to a strain of 0.07%. This is a magnified view of a part of Fig. 7.

Fig. 7 shows the fractional change in resistivity and the longitudinal stress/strain during static tensile loading up to failure. The resistivity increased monotonically with increasing strain up to failure. At a strain of 0.08% (just before failure), the resistivity increased abruptly. The behavior before the abrupt resistivity increase is shown in Fig. 8. The resistivity gradually increased with strain up to a strain of 0.05%.

The tensile properties are shown in Table IV. The stress-strain curve, as shown in Figs 7 and 8, is linear up to a strain of 0.04%. The slope of the curve decreased as the strain exceeded 0.04%, presumably due to plastic deformation. At a strain of 0.05%, the resistivity started to increase sharply without a significant change in the slope of the stress-strain curve (Fig. 8). This is presumably due to minor damage.

Fig. 9 shows the variation of the resistance during cyclic loading at a stress amplitude of 1.1 MPa. The specimen had not been loaded prior to this test. The resistance increased reversibly with strain in every cycle. The gage factor is $+0.63 \pm 0.08$. Fig. 10 shows the variation of the resistivity, as obtained by using the data in Fig. 9. The resistivity decreased reversibly with strain, though the noise was considerable. The fractional change in resistivity per unit strain is -0.39.

Fig. 11 shows the variation of the resistance during cyclic loading at a stress amplitude of 2.2 MPa. The specimen had not been loaded prior to this test. Both the resistance and strain increased reversibly upon loading at every cycle, except that only partial reversibility was observed in the first cycle. In cycles after the first cycle, the gage factor is $+1.84 \pm 0.13$ (Table III). The noise level was less than in Fig. 9. The behavior was similar in trend for the resistance (Fig. 11) and the resistivity (Fig. 12). The fractional change in resistivity per unit strain is $+1.13$.

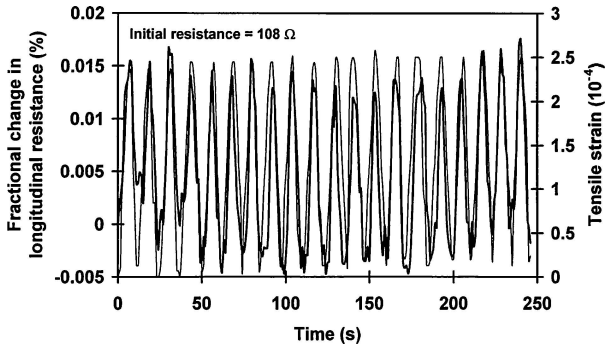

Figure 9 Variation of the fractional change in longitudinal resistance (thick curve) with time and of the tensile strain (thin curve) with time during cyclic loading at a stress amplitude of 1.1 MPa for the composite with both carbon fiber and carbon black.

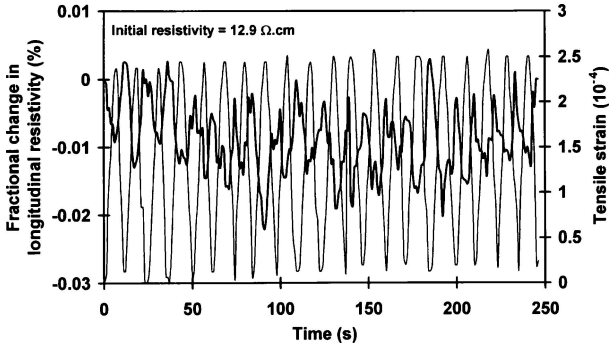

Figure 10 Variation of the fractional change in longitudinal resistivity (thick curve) with time and of the tensile strain (thin curve) with time during cyclic loading at a stress amplitude of 1.1 MPa for the composite with both carbon fiber and carbon black.

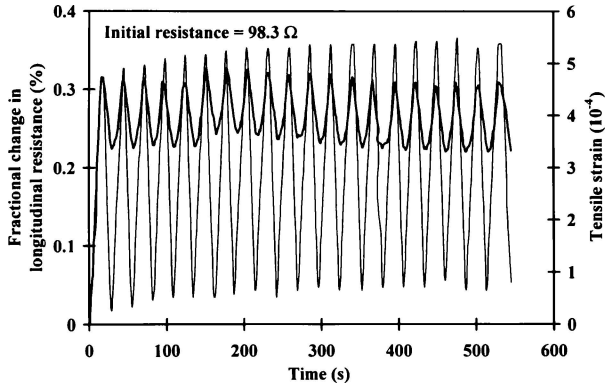

Figure 11 Variation of the fractional change in longitudinal resistance (thick curve) with time and of the tensile strain (thin curve) with time during cyclic loading at a stress amplitude of 2.2 MPa for the composite with both carbon fiber and carbon black.

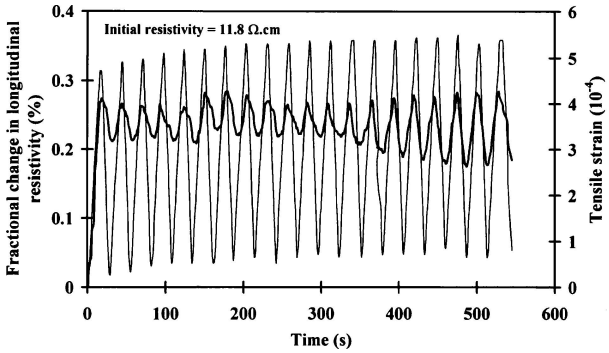

Figure 12 Variation of the fractional change in longitudinal resistivity (thick curve) with time and of the tensile strain (thin curve) with time during cyclic loading at a stress amplitude of 2.2 MPa for the composite with both carbon fiber and carbon black.

3.3.3. Summary of self-sensing and tensile behavior

For the composite with both carbon fiber and carbon black (Section 3.3.2), at a low tensile stress/strain amplitude (Figs 9 and 10) the piezoresistivity is very weak and slightly negative (i.e., the resistivity decreasing slightly with increasing tensile strain). However, at a high stress/strain amplitude (Figs 11 and 12), the piezoresistivity is weakly positive. At any stress/strain amplitude, the piezoresistivity is weak. In contrast, for the composite with carbon fiber as the sole filler (Section 3.3.1), the piezoresistivity is positive (i.e., the resistivity increasing with increasing tensile strain) at all stress/strain amplitudes, with the gage factor as high as 17 (higher for a stress amplitude of 2.2 MPa than that of 1.1 MPa). Thus, the strain self-sensing ability is superior for the case in which carbon fiber is the sole filler. The trend of positive piezoresistivity is as previously reported for a carbon black polyethylene-matrix composite and attributed to the change in separation between the neighboring filler particles [2].

The ductility (strain at failure) is 0.08% for the composite with both carbon fiber and carbon black, and is 0.09% for the composite with carbon fiber as the sole filler; the tensile strength is 3.3 MPa for the former, and is 3.6 MPa for the latter; the tensile modulus is 4.4 GPa for the former, and is 5.0 GPa for the latter (Table IV). Thus, the strength, modulus and ductility are all higher for the case of carbon fiber being the sole filler.

3.3.4. Softening temperature

As shown in Ref. 6, the softening temperature increases with carbon black volume fraction in the absence of carbon fiber. In this work, comparison of the softening temperatures for various ratios of carbon fiber to

carbon black at a total filler volume fraction of around 5% shows that the softening temperature is not much affected by the proportion of carbon fiber to carbon black. Both carbon black and carbon fiber increased the softening temperature from the value of 40.1°C [7] for the pitch matrix.

3.3.5. Dynamic mechanical properties

Table I shows that the flexural storage modulus is increased by the addition of carbon fiber and/or carbon black, as expected. The loss tangent (tan δ) is decreased by the addition of carbon black, but increased by the addition of carbon fiber or the addition of both carbon fiber and carbon black. The highest value of the loss tangent was attained by using carbon fiber as the sole filler. In spite of the high specific surface area of carbon black compared to carbon fiber, carbon black is not effective for enhancing the loss tangent. The origin of this behavior is presently not clear.

A high value of the loss tangent is attractive for vibration damping, while a high value of the storage modulus is attractive for stiffness. Thus, carbon fiber is attractive for both vibration damping and stiffness.

4. Conclusion

Pitch-matrix composites with carbon fiber as the sole filler are effective for the self-sensing of strain. The electrical resistivity increases reversibly with increasing tensile strain, with the gage factor as high as 17. Pitch-matrix composites with both carbon fiber and carbon black are less effective for strain sensing and lower in tensile strength, modulus and ductility than the composites with carbon fiber as the sole filler, but they are lower in the electrical resistivity. Pitch-matrix composites with carbon black as the sole filler are very high in the electrical resistivity and are rather low in the loss tangent, but they exhibit high storage modulus. The addition of either carbon fiber or carbon black to pitch increases the storage modulus, decreases the electrical resistivity, renders the ability to provide EMI shielding, and increases the softening temperature.

References

1. S. P. WU, L. T. MO and Z. H. SHUI, *Key Eng. Mater.* **249** (Composite Materials III) (2003) 391.
2. X. W. ZHANG, Y. PAN, Q. ZHENG and X. S. YI, *Polym. Int.* **50** (2001) 229.
3. D. DERWIN, P. BOOTH, P. ZALESKI, W. MARSEY and W. FLOOD, Jr., "Snowfree® Heated Pavement System to Eliminate icy Runways," FAA Icing & Deicing Conference, Paper 2003-01-2145, Society of Automotive Engineers (2003) p. 8.
4. S. WU, L. MO, Z. SHUI and Z. LIN, "Electric-Conductive Asphalt Concrete and Its Preparation Process," Faming Zhuanli Shenqing Gongkai Shuomingshu (2003) p. 8.
5. T. SAITO, K. HARAKAWA and T. KUNISHIMA, "Granular Binder Containing Electromagnetic Wave Absorber and Manufacture of Structural Article Using the Binder," Jpn. Kokai Tokkyo Koho (2001) p. 12.
6. T. KUNISHIMA, *Kogyo. Zairyo.* **50**(12) (2002) 34.
7. S. WEN and D. D. L. CHUNG, *Carbon* **42**(12/13) (2004) 2392.
8. P. W. CHEN and D. D. L. CHUNG, *Smart. Mater. Struct.* **2** (1993) 22.
9. X. SHUI and D. D. L. CHUNG, *J. Mater. Sci.* **35** (2000) 1773.

Received 30 November 2004
and accepted 22 February 2005